To be published in the Optical Polarimetry, Instrumentation and Applications; Society of Photo-Optical Instrumentation Engineers, Bellingham, Washington, Proceedings Vol. 112 (1977)

ELLIPSOMETRY OF ELECTROCHEMICAL SURFACE LAYERS

Rolf H. Muller

June 1977

Prepared for the U. S. Energy Research and Development Administration under Contract W-7405-ENG-48

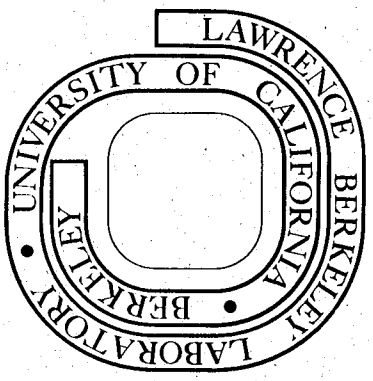

Optical Polarimetry, Instrumentation and Applications, Soc. Photo-Opt. Instr. Engrs., Bellingham, Wash., Proc. Vol. 112 (1977).

LBL-6617

Ellipsometry of Electrochemical Surface Layers

ROLF H. MULLER

JUNE, 1977

LBL-6617

Ellipsometry of Electrochemical Surface Layers

Rolf H. Muller

Materials and Molecular Research Division
Lawrence Berkeley Laboratory
and
Department of Chemical Engineering
University of California
Berkeley, California 94720

ABSTRACT

The measurement of changes in the state of polarization of light due to reflection provides an unusually sensitive tool for observing surface layers in any optically transparent environment. A fast, self-compensating ellipsometer has been used to observe the electrochemical formation of reacted surface layers. The optical effect of mass-transport boundary layers and component imperfections have been taken into account in the interpretation of results.

INTRODUCTION

Ellipsometry is concerned with the analysis and interpretation of changes in the state of polarization caused by reflection.[1,2] The technique has found increasing interest in recent years[3-5] for the measurement of thin films because it is unusually sensitive, disturbs the object minimally and can be applied to surfaces contained in any optically transparent medium. Film thicknesses amenable to measurement range from fractional monoatomic coverage to microscopic thicknesses.

PRINCIPLES

Two parameters are normally measured in ellipsometry.[6] They can be expressed as the difference in phase Δ and the change in the ratio of amplitudes of p and s components $\tan \psi$ introduced by the reflection. With some instruments, changes in reflectivity can also be measured[7] and thus a third parameter is available for the interpretation, which often requires the determination of more than two unknown quantities. Definitions and conventions established previously[8] will be used here.

Two factors are primarily responsible for the high resolution of the technique: The first reason is that two components of the electromagnetic field are measured against each other, and relative measurements are inherently more accurate than absolute measurements. The second reason is that azimuth angles are usually measured and angle measurements can be made rather easily with high precision.

PURPOSE

Electrochemical surface layers will be considered here. These are formed by chemical reactions in which the rate is electrically monitored or controlled. Compared to the chemical formation of surface layers, additional measured parameters available for the interpretation are the potential, which indicates thermodynamically feasible reactions, and charge which indicates amount of product formed.

Of immediate interest are layers formed in the charge and discharge of batteries and in the electrochemical deposition and dissolution of metals. Surface layers also determine the chemical properties of metals in most practically important environments. They are formed in corrosion processes[9] and have been shown to change the reactivity of metals by as much as nine or ten orders of magnitude.[10]

Physically adsorbed surface layers of ions and molecules, which are thinner than most reacted layers, can also be observed by ellipsometry.[9] Adsorption from a liquid phase, however, seems to be more difficult to interpret[11] than adsorption from the vapor phase.[12,13]

The attractiveness of ellipsometry for the observation of electrochemical interfaces stems primarily from its capability for in situ measurements: Surfaces do not need to be exposed to environments, such as vacuum or electron impact, that could alter their properties. Also, electrical measurements can be

conducted simultaneously. Ellipsometer measurements are primarily sensitive to the amount of material present in a surface layer; in addition, they are also sensitive to the topography.

INSTRUMENTATION

Ellipsometer instrumentation is presently in a state of rapid development. Manually operated ellipsometers are of the compensating type in which linear polarization is restored and extinction accomplished. Different arrangements of optical components can be used for this purpose.[6]

Automatic ellipsometers have been introduced to provide more rapid response and greater resolution than that possible with manual operation. Principles and performance of automatic instruments have been reviewed recently.[14] They can be of a compensating or a non-compensating type. In the former, an error signal is derived from the response of the transmitted irradiance to a modulation of azimuth or phase and used to drive a servo loop to compensation. In the latter, the state of polarization is derived from the response of the irradiance at the detector to a modulation in azimuth or phase.

The fastest response and the highest resolution obtained so far with both types of instruments are quite similar. Compensating ellipsometers can be expected to be more accurate, non-compensating ellipsometers are more easily adapted for wavelength scanning.[14]

The self-compensating ellipsometer used in this work has been built primarily for following electrochemical film formation proceeding on metal electrodes at rates of practical interest. It allows the observation of rapid, large changes on surfaces with moderate resolution, or slow, small changes with high resolution.

Principles of operation and details of construction have been described previously.[15] Figure 1 indicates the arrangement of components, and the operating principles are summarized in Table I. Modulation and compensation are accomplished by electronic azimuth rotation of polarizer and analyzer with Faraday cells. The electrically-measured azimuth readings are added to the mechanically-set positions of polarizer and analyzer prisms and are simply related (for ideal optical components) to relative phase and amplitude change in reflection.[6]

The optical ellipsometer components are mounted in two sub-assemblies which allow one to convert to the use of vertical or horizontal specimen surfaces (facing up or down) without alignment of individual components. A configuration with a horizontal surface facing down is shown in Fig. 2.

The performance characteristics of the ellipsometer are summarized in Table II. They are those determined previously with a rapidly varying specimen surface,[16] except for the dynamic range, that has been doubled since by the use of new compensating power supplies.

INTERPRETATION

The optical components of ellipsometers generally contain imperfections, such as strain-induced birefringence, dichroism, deviation from quarter-wave retardation, or misalignment of azimuth circles. Such imperfections are recognized by differences in results obtained from measurements in different zones[6] when the relations valid for ideal components are used. Compared to a manually operated ellipsometer with a specimen in air, the instrument used here employs a larger number of optical components (Faraday cores, chamber windows). It is therefore even more desirable to account for their imperfections.

A previous analysis for manually operated ellipsometers[17] has been extended to include the Faraday cell cores.[18] A matrix notation has been used to represent the optical effect of individual components, and imperfections are treated as first-order Taylor series expansions about the ideal values. In a calibration procedure, 26 measurements are performed from which 19 imperfection parameters are computed. For measurements which range over only a few degrees in Δ and ψ, the corrections have been found to consist of additive constants, as illustrated in Fig. 3, over a larger range, the magnitude of the correction is not constant and may even change sign (Fig. 4).

The electrochemical formation of surface layers at appreciable rates is unavoidably associated with the depletion or

accumulation of reactants and products in the liquid phase near the solid surface. An investigation of the effect of such optically inhomogeneous mass-transport boundary layers on the observation of surface layers by ellipsometry has shown that their effect can be significant.[19] It depends strongly on angle of incidence and optical constants of the substrate (Fig. 5). For refractive-index gradients typically encountered in electrochemical boundary layers, the optical effect depends on the refractive index of the solution in the homogeneous (bulk) part and at the interface, but is independent of the thickness of the boundary layer and the exact nature of the refractive-index profile in it. This rather unexpected behavior shows that homogeneous films, in general, cannot be used to represent boundary layer effects. The physical reason for the optical behavior is that reflection from within the inhomogeneous film is negligible and the principal effect of the boundary layer is a change in the angle of incidence at the electrode surface.

The interpretation of film properties has been based on the classical Drude equation for isotropic, linear materials. According to this model, films are assumed to be of uniform thickness, bounded by parallel faces. The interpretation provides an equivalent thickness, which is a measure of the amount of materials present, irrespective of its geometrical distribution, and a refractive-index, which is indicative of the nature and porosity of the film material.

Great advances have recently been made in understanding the ellipsometry of birefringent films and substrates,[20,21] but no general study of birefringence of films has been attempted in this work yet. Uniaxial birefringence has been found not to account for the observations. A more general analysis will be undertaken in connection with film growth experiments on single crystals, presently in progress.

Although many ellipsometer measurements, when considered singly, lead to a large (even infinite) number of possible interpretations, requirements of continuity as a function of time often allow one to exclude extraneous solutions. Electrochemical information on the nature and amount of film material formed and mass-transport considerations can further restrict uncertainties in interpretation. The combined use of all the information available will be discussed in a separate paper at this meeting.

APPLICATIONS

The analysis of boundary layer effects has resulted in the establishment of ellipsometry as a new technique for the determination of interfacial concentration at electrodes in liquids. Such measurements complement interferometer observations[22] which typically provide the boundary layer thickness more precisely than the interfacial concentration.

Results from a determination of interfacial concentration during metal deposition in a flow channel are shown in Fig. 6. The optical effects of changes in surface roughness have been separated from those due to the boundary layer by the use of current pulses. The close agreement of the ellipsometer measurements with empirical correlations, shown as dashed and solid lines for the laminar and turbulent regimes, illustrate the validity of the technique.[18]

The ellipsometry of solid electrochemical surface layers, in general, requires the simultaneous consideration of many possible processes and the full capabilities of the equipment. A special example, in which different optically dominant processes are observed in sequence, is illustrated in Fig. 7. Starting from the locus of the bare zinc, the measurements first indicate a roughening of the surface up to an equivalent peak-peak roughness of about 100 Å (square ridge Model[23]). Dissolved reaction products are then observed to accumulate in a mass-transfer boundary layer until a concentration close to saturation is reached at the interface. The growth of a solid film, which electrical measurements show to be passivating, then sets in. The computed points, which the measurements reasonably follow for the lower film thicknesses (shown with the points), indicate that the film is optically absorbing, probably caused by oxygen deficiency in the oxide.

A more complex series of events is illustrated in Fig. 8 for the anodic oxidation of silver. Potential measurements indicate that segment Ia of the computed curve represents the growth of an Ag_2O layer. The existence of what we have called a colloidal overlayer has to be assumed, however, to reproduce the measurements satisfactorily. A shift in potential indicates a gradual change of film composition during the growth represented by segment Ib. Conversion of the entire film to AgO, accompanied by a rapid change in potential, occurs in segment II and can also be approximated by computation.

In order to justify assumptions made in the interpretation of a reasonably complex film formation, such as the one above, two questions must be resolved: The first is whether the derived optical properties of the surface represent a unique interpretation; the second is whether physical and chemical properties derived from the optical data can be supported by independent experimental evidence. The uniqueness of the optical computations can be tested by an automated search for other possible solutions. In order to keep the computational effort within acceptable limits, however, it is usually necessary to restrict the search to specific film models, as will be discussed separately.

Independent experimental evidence of film properties is now being obtained by a newly-built combination of ellipsometry with ion etching and Auger spectroscopy for films that

have been transferred to vacuum. In particular, it is hoped that profiles of composition and porosity across films and multiple-layer film structures[24] can thus be determined.

OUTLOOK

Recent instrumental developments in ellipsometry have opened large fields of application that are still being defined. The systematic use of spectroscopic ellipsometry[25] in particluar is adding a new dimension to the technique. The experimental capabilities are, however, now ahead of the theoretical base of interpretation in several respects. Two problems which continue to present serious obstacles in the present context are surface roughness and patchwise film distribution (or locally varying thickness). Additions to recent theoretical work[26,27] and comparison with carefully exexuted experiments are very much needed.

ACKNOWLEDGEMENT

This work was conducted under the auspices of the U.S. Energy Research and Development Administration.

TABLE I

Components of Fast, Self-Compensating Ellipsometer

Light Source	-	100W high-pressure mercury short-arc, stabilized power supply, condenser.
Filter	-	Narrow-band interference filter (546 ± 5 nm), i.r.-absorbing filter.
Collimator	-	Pinhole entrance 1 mm, f = 260 mm.
Polarizer	-	Glan-Thompson prism in divided circle, resolution 0.01°.
Polarizer Faraday Cell	-	Separate modulation and compensation solenoids.
Compensator	-	Mica quarter wave plate in divided circle, resolution 0.10°.
Specimen	-	Contained in liquid or vacuum chamber.
Analyzer Faraday cell	-	Separate modulation and compensation solenoids.
Analyzer	-	Glan-Thompson prism in divided circle.
Telescope	-	Pinhole exit 1 mm, f = 260 mm.
Photodetector	-	Photomultiplier RCA 931A.
Modulation	-	Polarizer and analyzer, ± 0.9° 10 kHz.
Compensation	-	Polarizer and analyzer azimuth, ± 55°.

TABLE II

Performance characteristics of fast, self-compensating ellipsometer (fast mode: time constant 0.001s, slow mode: time constant 0.1s, preliminary data).

	Δ	ψ
Slew rate, fast mode:	3,200°/s	1,600°/s
Slew rate, slow mode:	0.66°/s	0.33°/s
Resolution, fast mode:	0.08°	0.04°
Resolution, slow mode:	0.0014°	0.0007°
Dynamic range:	200°	110°
Cross-modulation for change of ± 5° in ψ or ± 10° in Δ:	± 0.004°	± 0.002°
Cross-modulation for change of ± 100° in ψ or ± 200° in Δ:	± 0.04°	± 0.02°

FIGURE CAPTIONS

Fig. 1 - Block diagram of fast, self-compensating ellipsometer.

Fig. 2 - Optical components of ellipsometer arranged for use of horizontal specimen surface facing down. Light propagation from left to right.

Fig. 3 - Correction of ellipsometer imperfections. Growth of zinc oxide film on zinc. 0.5 M KOH, - 1.0 V vs. Hg/HgO.

Fig. 4 - Correction for ellipsometer imperfections. Growth of zinc oxide film on zinc. 0.5 M KOH, - 1.2 V vs. Hg/HgO.

Fig. 5 - Effect of substrate refractive index n-ik on the change in relative phase caused by the presence of a dissolution mass-transport boundary layer with refractive index difference 0.03 (approximately 1 M concentration difference), angle of incidence 70°.

Fig. 6 - Interfacial concentration determined by ellipsometry (copper deposition from 0.1 M $CuSO_4$ in a flow channel) as a function of Reynolds number for different current densities.

Fig. 7 - Different optically dominant effects in the ellipsometry of anodic film formation: Surface roughening, build-up of boundary layer and solid film precipitation. Zinc in 0.5 M KOH.

Fig. 8 - Anodic oxidation of silver. Segments of computed curve. Ia: Ag_2O, n = 1.8 - 0.50i; Ib: Gradual change to n = 1.76 - 0.56i (partial AgO); II: film conversion to n = 1.9 - 0.70i (AgO). Colloidal overlayer: n = 1.45, 1,200 Å.

REFERENCES

1. A. C. Hall, Surf. Sci., 16, 1 (1969).
2. R. M. A. Azzam, Surf. Sci., 56, 6 (1976).
3. Ellipsometry in the Measurement of Surfaces and Thin Films, Symposium proceedings, September 5-6, 1963, edited by E. Pasaglia, R. R. Stromberg and J. Kruger, National Bureau of Standards, Misc. Publ. 256 (1964).
4. Recent Developments in Ellipsometry, Proceedings of Symposium, August 7-9, 1968, edited by N. M. Bashara, A. B. Buckman and A. C. Hall, also Surf. Sci., 16, (1969).
5. Proceedings of Third International Conference on Ellipsometry, September 23-25, 1975, edited by N. M. Bashara and R. M. A. Azzam, also Surf. Sci., 56, (1976).
6. R. H. Muller, Principles of Ellipsometry, in Advances in Electrochemistry and Electrochemical Engineering, Vol. 9, edited by R. H. Muller, Wiley-Interscience, New York, 1973.
7. J. Horkans, B. D. Cahan and E. Yeager, J. Electrochem. Soc., 122, 1585 (1975); B. D. Cahan, Surf. Sci., 56, 354 (1976).
8. R. H. Muller, Surf. Sci., 16, 14 (1969).
9. J. Kruger, Applications of Ellipsometry to Electrochemistry, in Advances in Electrochemistry and Electrochemical Engineering, Vol. 9, edited by R. H. Muller, Wiley-Interscience, New York, 1973.

10. D. A. Vermilyea, Phys. Today, 29, 23 (1976).

11. B. E. Conway, H. Angerstein and L. H. Laliberté, J. Electrochem. Soc., 121, 1596 (1974); W. Paik, M. A. Genshaw and J. O' M. Bockris, J. Phys. Chem., 74, 4266 (1970).

12. R. H. Muller, R. F. Steiger, G. A. Somorjai and J. M. Morabito, Surf. Sci. 16, 234 (1969); Surf. Sci., 14, 279 (1969).

13. F. Meyer, E. E. DeKluizenaar and G. A. Bootsma, Surf. Sci., 27, 88 (1971); F. Meyer, Surf. Sci., 56, 37 (1976).

14. R. H. Muller, Surf. Sci., 56, 19 (1976).

15. H. J. Mathieu, D. E. McClure and R. H. Muller, Rev. Sci., Instrum. 45, 798 (1974).

16. R. H. Muller and H. J. Mathieu, Appl. Opt., 13, 2222 (1974).

17. R. M. A. Azzam and N. M. Bashara, J. Opt. Soc. Am., 61, 773 (1971).

18. C. G. Smith, Ph.D. Thesis, in preparation.

19. R. H. Muller and C. G. Smith, Surf. Sci., 56, 440 (1976).

20. D. Den Engelsen, Surf. Sci., 56, 272 (1976).

21. D. J. DeSmet, J. Opt. Soc. Am., 65, 542 (1975).

22. F. R. McLarnon, R. H. Muller and C. W. Tobias, J. Opt. Soc. Am., 65, 1011 (1975); R. H. Muller, Electrochim. Acta, in press.

23. C. A. Fenstermaker and F. L. McCrackin, Surf. Sci., 16, 85, (1969).

24. J. L. Ord and D. J. DeSmet, J. Electrochem, Soc., 123, 1876 (1976).

25. D. E. Aspnes, Spectroscopic Ellipsometry of Solids, in Optical Properties of Solids, Vol. 2, edited by B. O. Seraphin,, North-Holland, Amsterdam, 1976; D. E. Aspnes and A. A. Studna, Appl. Opt. 14, 220 (1975).

26. I. Ohlidal and F. Lukes, Optica Acta, 19, 817 (1972).

27. H. Raether, Thin Solid Films, 28, 119 (1975).

Fig. 1

XBL 777-1287

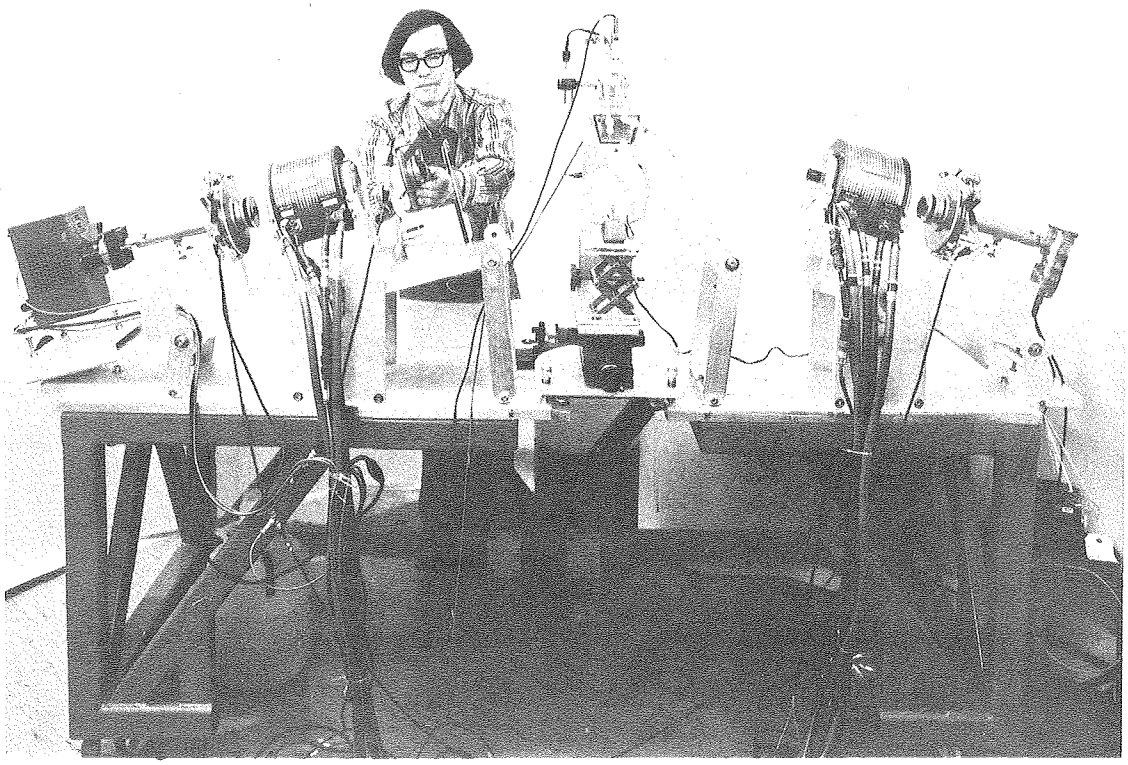

CBB 750-7285

Fig. 2

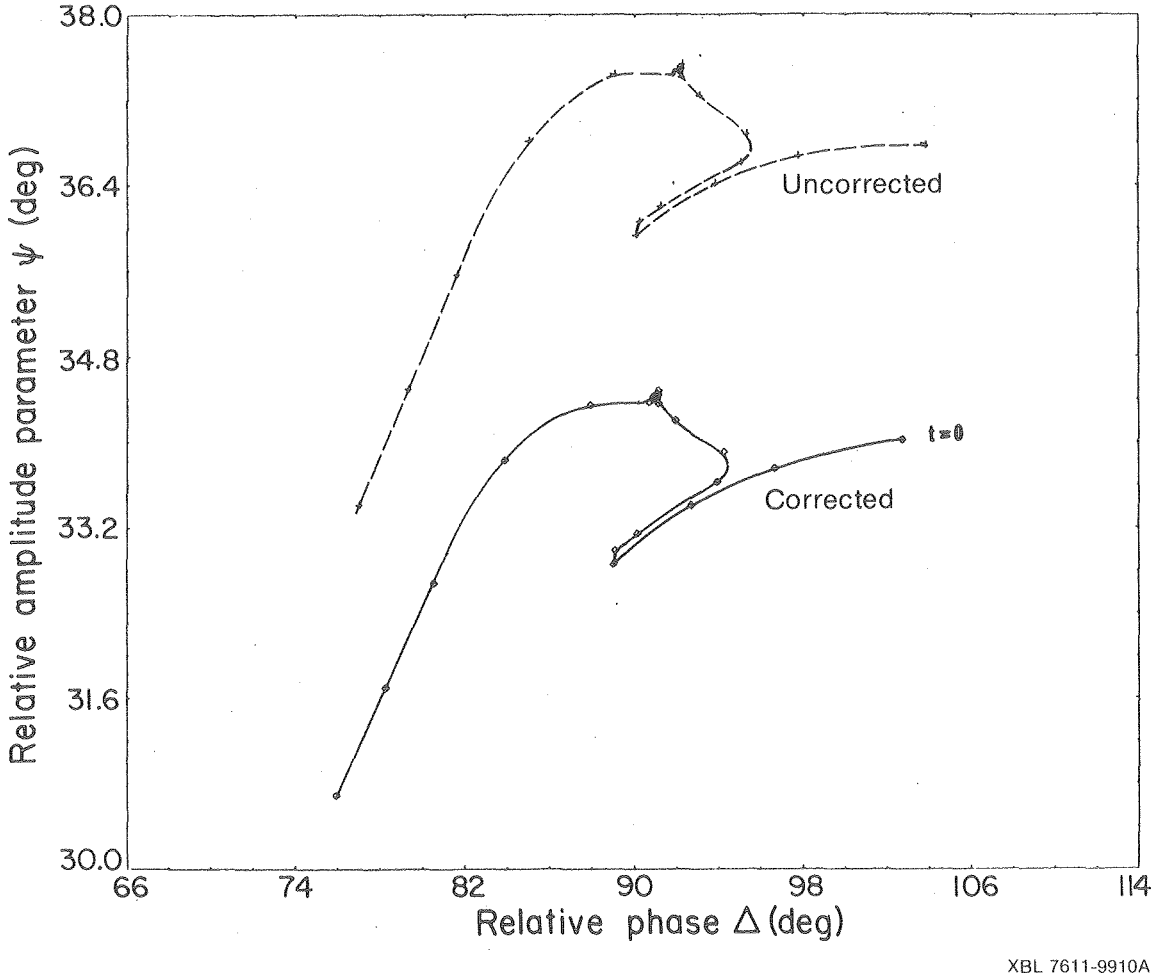

Fig. 3

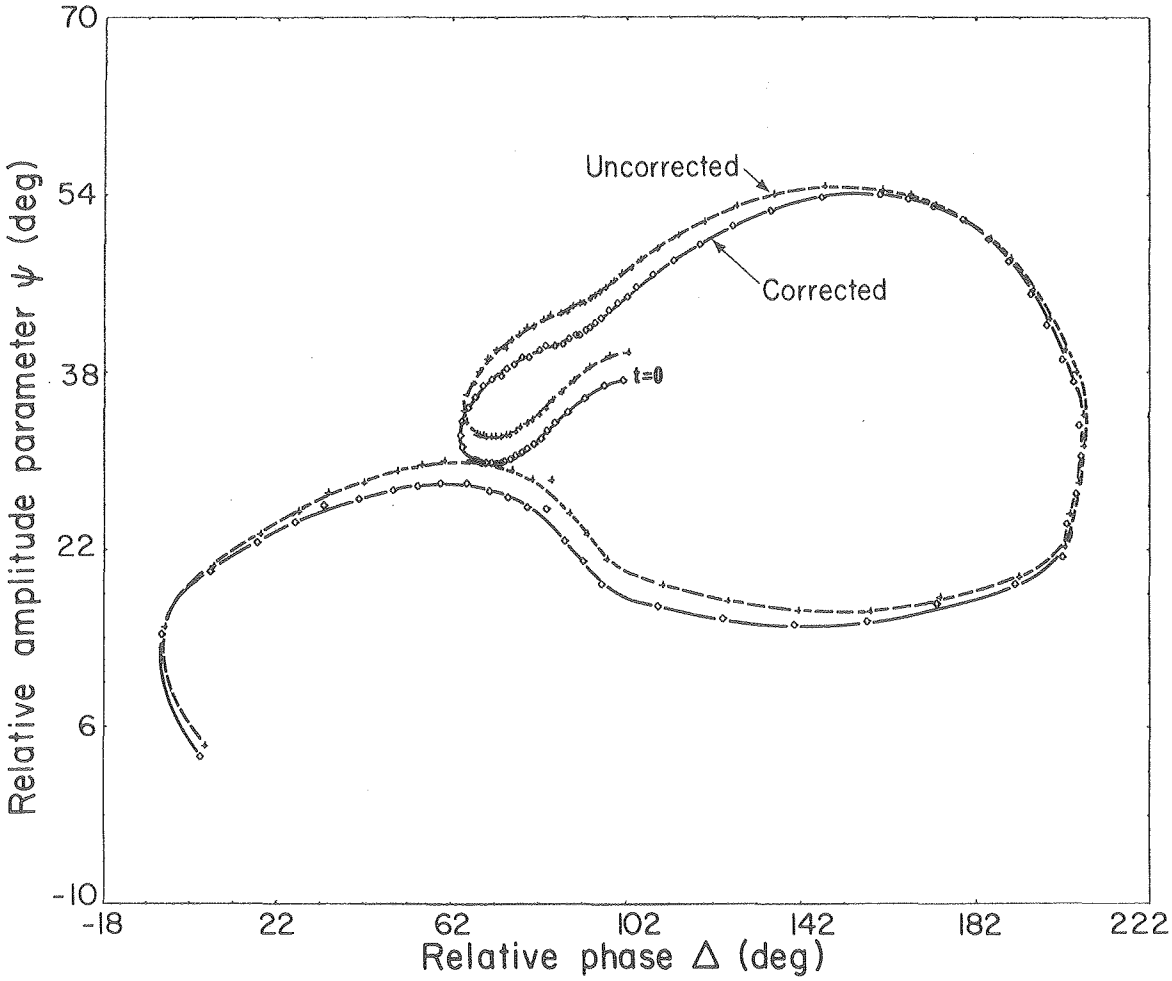

XBL 7611-9909A

Fig. 4

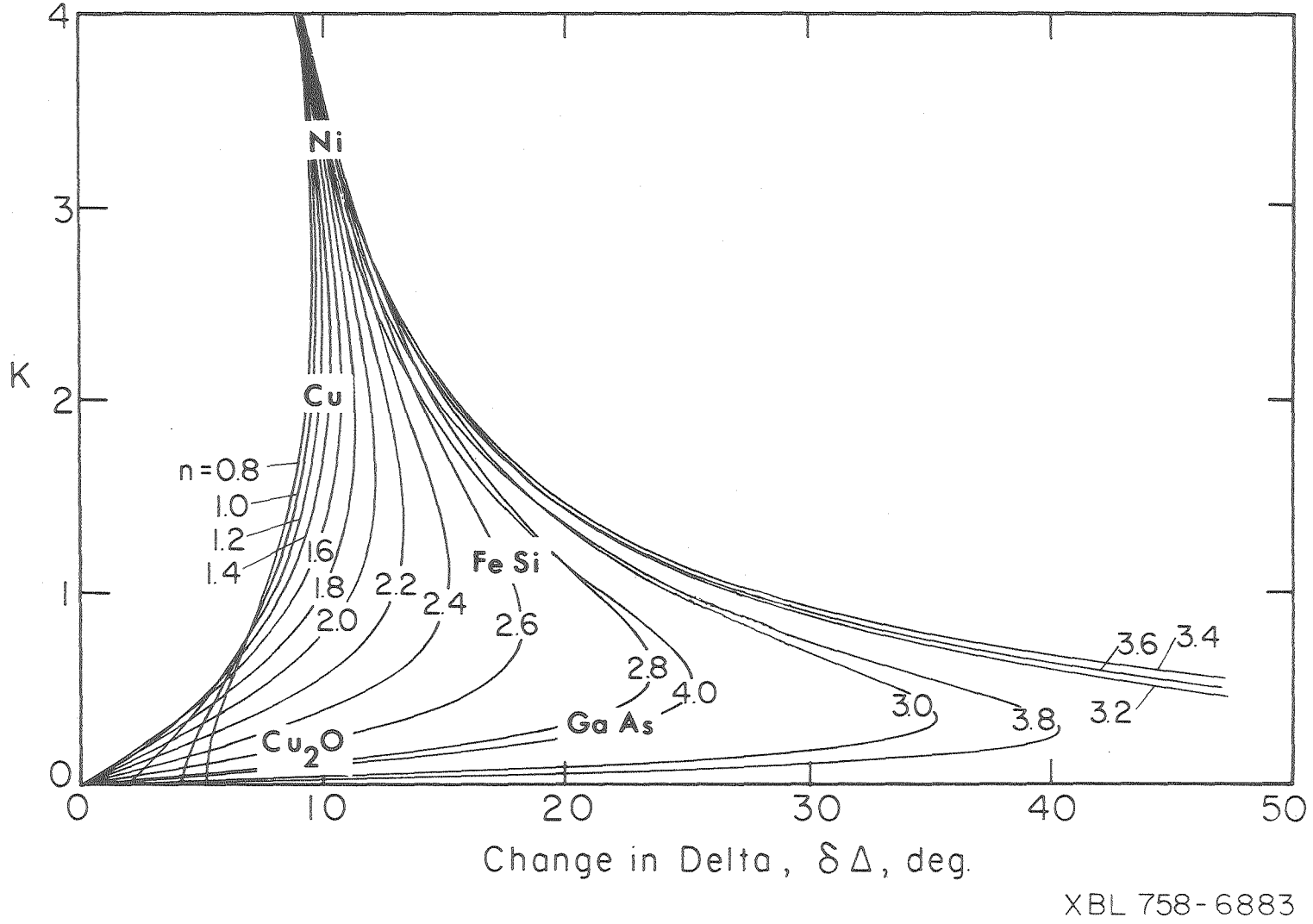

XBL 758-6883

Fig. 5

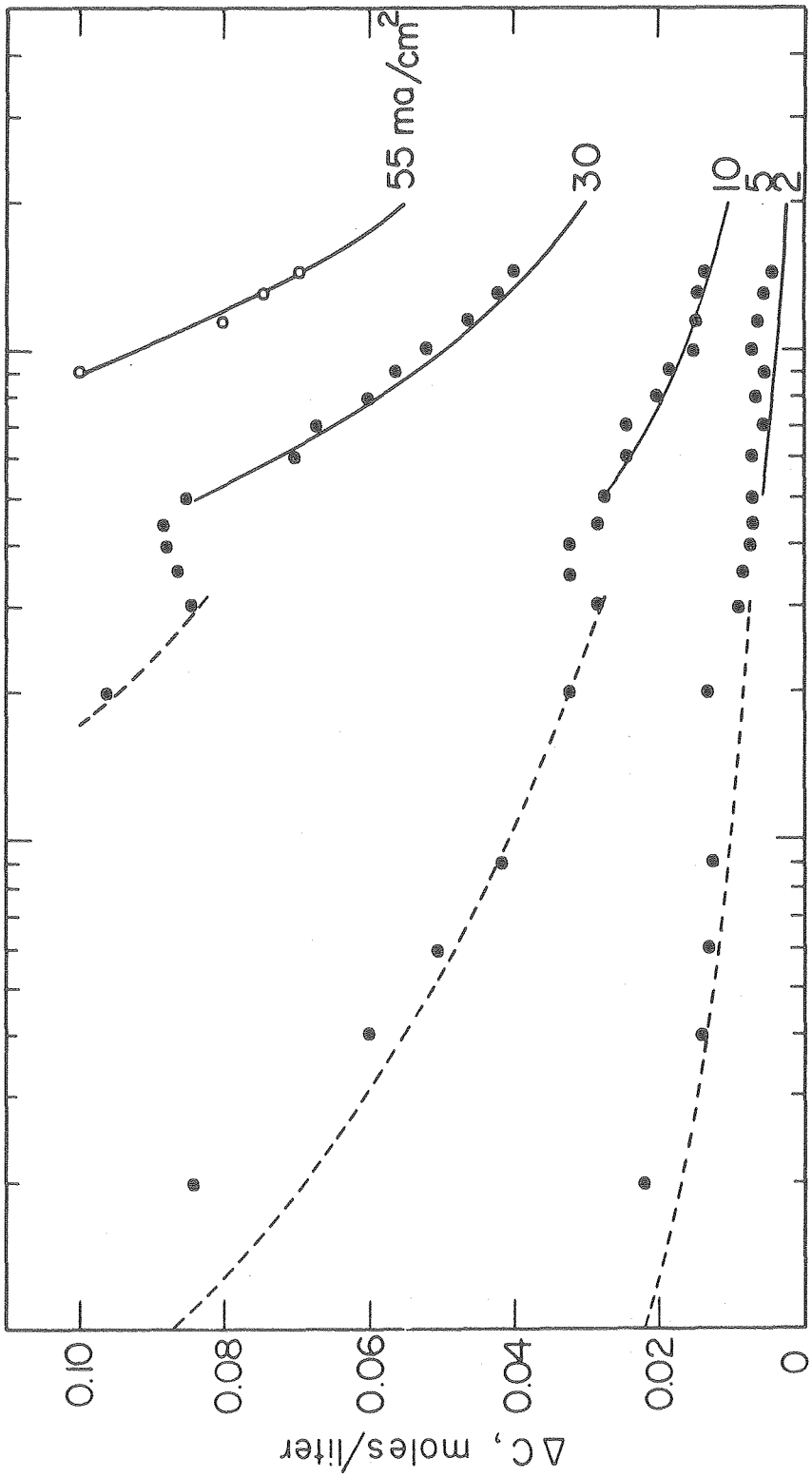

XBL758-6892B

Fig. 6

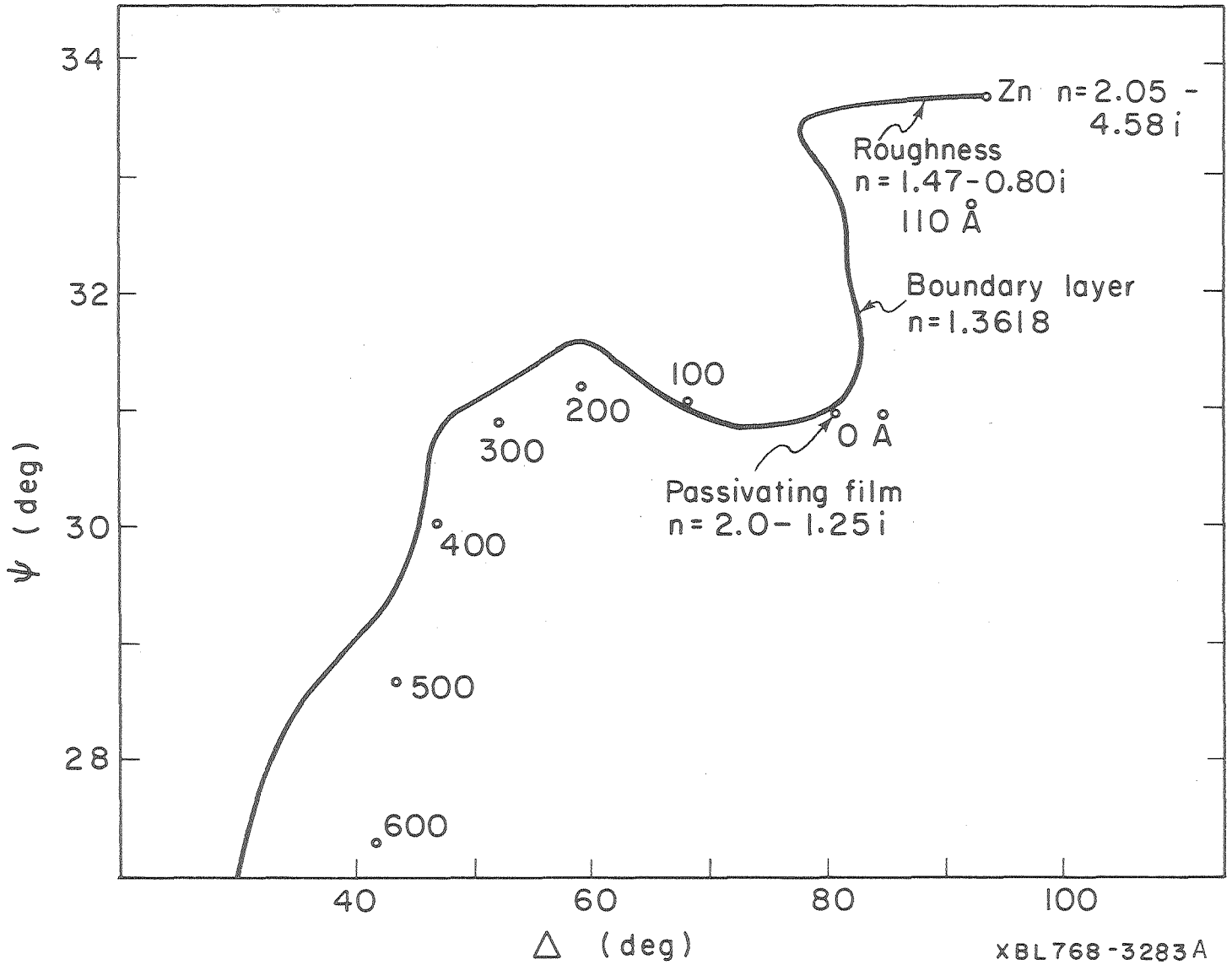

Fig. 7

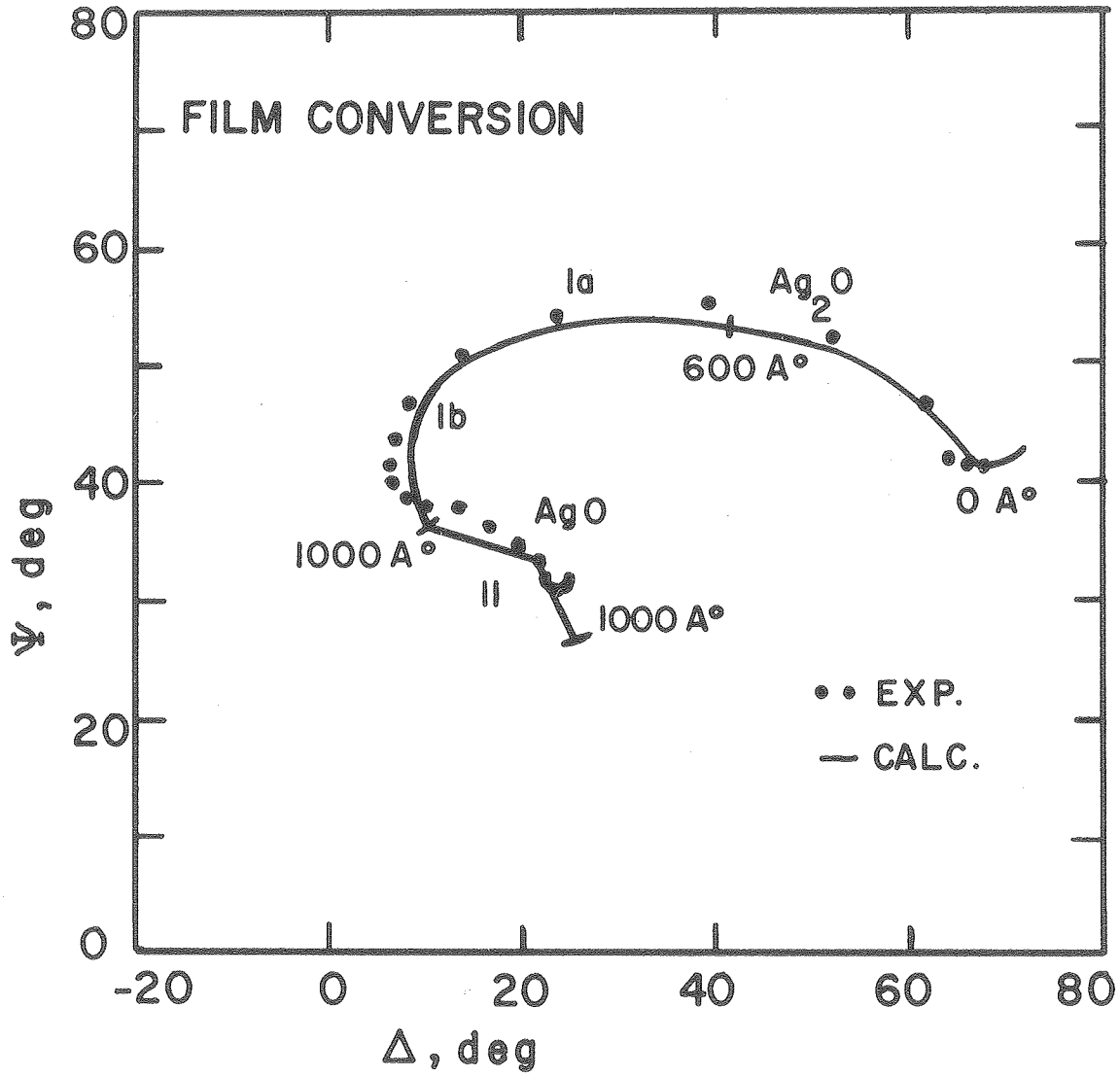

XBL 772-7541 A

Fig. 8

This report was done with support from the United States Energy Research and Development Administration. Any conclusions or opinions expressed in this report represent solely those of the author(s) and not necessarily those of The Regents of the University of California, the Lawrence Berkeley Laboratory or the United States Energy Research and Development Administration.